IEEE Access
Multidisciplinary | Rapid Review | Open Access Journal

Received December 22, 2018, accepted January 26, 2019, date of publication February 7, 2019, date of current version February 27, 2019.

Digital Object Identifier 10.1109/ACCESS.2019.2898029

Dependence of the Perceptual Discrimination of High-Frequency Vibrations on the Envelope and Intensity of Waveforms

NAN CAO[1], (Student Member, IEEE), MASASHI KONYO[1], (Member, IEEE), HIKARU NAGANO[2], (Member, IEEE), AND SATOSHI TADOKORO[1], (Fellow, IEEE)

[1]Graduate School of Information Sciences, Tohoku University, Sendai 980-8579, Japan
[2]Graduate School of Engineering, Kobe University, Kobe 657-8501, Japan

Corresponding author: Nan Cao (cao.nan@rm.is.tohoku.ac.jp)

This work was supported in part by the ImPACT Program "Tough Robotics Challenge," and in part by the Japan Society for the Promotion of Science (JSPS) Grants-in-Aid for Scientific Research Program (KAKENHI) Grant Number JP18H01401.

ABSTRACT Humans perceive and discriminate high-frequency tactile vibrations based on the intensity and envelope of the stimuli. However, no studies have investigated exactly how the envelope and intensity each affect the ability to discriminate. The objectives of this paper are to identify the boundary at which the envelope begins not to strongly affect the ability to discriminate vibrations and to investigate the effects of the carrier frequency and intensity on the discrimination ability. The results of our testing showed that the ability to discriminate was dependent on the envelope frequency and that the ability to discriminate sinusoidal and amplitude-modulated (AM) vibrations in which the envelope frequency ranged from 12 to 50 Hz was higher than that required to discriminate sinusoidal and AM vibrations in which the envelope frequency was above 80 Hz. When the envelope frequency of an AM vibration was 125 Hz, the ability to discriminate sinusoidal and AM vibrations was found to be low and no significant difference was noted in comparison to discriminating AM vibrations with the same envelope frequency. These results suggest that the boundary for envelope perception was at an envelope frequency of around 80–125 Hz at low intensities and that the carrier frequency had little effect on the discrimination, although the discrimination ability tended to increase as the intensity increased.

INDEX TERMS Envelope frequency, intensity, high-frequency vibration, perceptual discrimination.

I. INTRODUCTION

To provide relevant haptic information to users, it is important to understand which and how high-frequency vibration factors, such as the frequency, amplitude, envelope, shape tactile perception of the various characteristics of objects and surfaces, including their similarity, roughness, and strength. High-frequency vibrations induced by scratching or tapping on surfaces has been identified in various studies as a cue for roughness or hardness perception [1]–[4]. Thus, the transmission of high-frequency vibrations has been attempted in the support of telerobotic surgery [5] and to deliver realistic textures [6], [7]. When rendering tactile vibrations, many applications have employed amplitude-modulated (AM) and/or frequency-modulated (FM) vibrations. For example, Ahmaniemi *et al.* [8] leveraged modulated vibrations to render the texture of a contact surface. In addition, image-based tactile vibration using modulated vibration have been used to render different contact surfaces in a flat tablet [9] and vibration patterns have been used to represent various notifications [10]. For example, decaying sinusoidal waves have been applied to the skin to indict roughness or collisions in a virtual environment [1], [11]. Vibration patterns are widely used for tactile generation in virtual reality (VR) environments [8] to facilitate the teleoperation of robots [12], [13]. Takenouchi *et al.* [14] extracted the envelope of a high-frequency vibration for which the carrier frequency was above the range of human perception.

The intensity of a high-frequency vibration (i.e., a vibration above 100 Hz), which is generally defined as the integral of the stimulus intensity over time or the spectral power summed across all frequencies, has been identified as a primary cue in the perception of vibrotactile information in the Pacinian system [15]–[18]. Makous *et al.* [15] found that the intensity

The associate editor coordinating the review of this manuscript and approving it for publication was Eunil Park.

model, which is a function of the spectral power divided by the threshold power, constitutes a measure of the ability to excite a Pacinian system. Bensmaïa *et al.* [17] developed a spectral model that improved on the intensity model by adding spectral characteristics based on psychophysical and neurophysiological findings and then applied that model to finely textured stimuli to infer perceptual dissimilarities [18].

However, it has been found that the intensity model is insufficient when interpreting the perception of the envelope of a high-frequency vibration. For example, in this model, two sinusoidal waves with slightly different frequencies will be perceived almost identically. If two vibrations are simultaneously generated at the same point, a subject is able to perceive the beat frequency and can even count the number of beats when the new superimposed waveform has a very slow envelope frequency. Lim *et al.* [19] found that humans can perceive beats for envelope frequencies from 2.5 to 10 Hz and the ratio between the beat detection $AT_B(f)$ and amplitude thresholds $AT(f)$ decreases from 20 to 1.25 as the carrier frequency increases from 63.1 to 398 Hz. These results indicate the beats can be perceived for very low envelope frequencies and become closer to the AT when f_c is increased. Humans can perceive the frequency of an amplitude modulated sinusoidal vibration even when the carrier frequency is above the range they can perceive [20], [21], which suggests that humans can perceive the envelope of high-frequency vibrations. Park and Choi [22] found that AM vibrations at a very high envelope frequency are similar to the sinusoidal vibration ($f_e = 0$), which suggests that when the envelope frequency is high, the beats cannot be perceived and the waveform is therefore perceptually similar to vibrations without an envelope frequency. Once these results were obtained, Park *et al.* did not investigate the boundary and intensity effect further.

The intensity and envelope of waveforms affects the ability of humans to discriminate high-frequency vibrations; however, the mechanism describing how the envelope perception and intensity interact is not yet clear. It is anticipated that an improved understanding of their effects will assist in the design of vibration devices for haptic functions in vibration rendering and communications applications.

The objectives of this study were to identify the boundary at which the envelope begins not to strongly affect the ability to discriminate vibrations and to investigate the effects of the carrier frequency and intensity on the discrimination ability. To accomplish this, psychophysical experiments were conducted using AM vibrations of different frequencies and intensities. Specifically, AM vibrations were compared with sinusoidal vibrations at different intensities to identify the similarities and differences between them, and vibrations of different envelopes and vibrations of the same envelope were compared to evaluate the effect of the envelope on the perception. Then, stimuli at different intensities were compared to investigate the effect of the intensity on the perception. Finally, we also investigated the effect of the carrier frequency on the ability to discriminate.

II. METHODS

A. AMPLITUDE-MODULATED VIBRATION

In this study, investigated the effects of the intensity and envelope of amplitude-modulated vibrations on human perception. The following equation was used to describe the AM vibrations:

$$q(t) = \mathrm{env}(t) \times \cos(2\pi f_c t), \tag{1}$$

where $env(t)$ is an envelope waveform and f_c is the carrier frequency.

The following describes one type of AM vibration:

$$q(t) = A\left(0.5 + 0.5\sin(2\pi f_e t - \frac{\pi}{2})\right)\sin(2\pi f_c t), \tag{2}$$

where A is the amplitude, f_e is the envelope frequency, and f_c is the carrier frequency.

This waveform can also be represented as:

$$\begin{aligned} q(t) = {} & 0.5A\sin(2\pi f_c t) + 0.25A\sin\left(2\pi\left(f_e - f_c\right)t\right) \\ & - 0.25A\sin\left(2\pi\left(f_e + f_c\right)t\right). \end{aligned} \tag{3}$$

From Eq. 2, the vibration is made up of an envelope signal and a carrier signal and is composed of three sinusoidal waves.

B. INTENSITY MODEL

In [17], the intensity model of a vibration consisting of one to three frequency components can be written as follows:

$$I(f) = \left[\left(\frac{A}{AT(f)}\right)^2\right]^{a(f)}, \tag{4}$$

where A is the amplitude of the waveform, f is the frequency, $AT(f)$ is the amplitude threshold, which is related to frequency f, and $a(f)$ is an exponent representing the scale of the intensity with respect to the frequency f. The units of I are $\left[\left(\frac{\mu m}{\mu m}\right)^2\right]^{a(f)}$, where $\frac{\mu m}{\mu m} = 1$ and $a(f)$ is a value. Thus, the units are equivalent to '1'. Note that the units are not shown in the following.

Bensmaïa *et al.* [17] used the intensity model to develop a spectral model that consisted of many minichannels characterized by a Gaussian filter with a center frequency f_c and standard deviation αf_c. The intensity of one channel (center frequency f_c) can be represented as follows:

$$Z_s(f_c) = \sum_f I(f) e^{-\frac{(f-f_c)^2}{2(\alpha f_c)^2}}. \tag{5}$$

C. STIMULI

In this experiment, the stimuli were defined as per Eq. 2 and each consisted of a combination of three parameters: the amplitude A, carrier frequency f_c, and envelope frequency f_e. The related intensity parameters of the sinusoidal wave, including the frequency f, amplitude threshold $AT(f)$, and exponent $a(f)$, are shown in Table 1. The amplitude threshold (AT) of the sinusoidal waves was measured via psychophysical experiments that applied the 1-up 2-down

TABLE 1. Amplitude thresholds and exponents of the sinusoidal waves for the different frequencies.

f [Hz]	$AT(f)$ [μm]	Exponent $a(f)$ [18]
100	0.25	0.65
150	0.17	0.6
200	0.18	0.51
300	0.18	0.52
400	0.20	0.34

staircase method as per the three-interval forced-choice procedure and the experiment involved five subjects. The mean values of the results are shown in Table 1.

In terms of the $AT(f)$, the values of the $AT(f)$ were fitted using the following equation based on the ATs in Table 1,

$$\log(AT(f)) = a + be^{-\frac{(f+c)^2}{d}}. \tag{6}$$

The AT(f) values after fitting are shown in Fig. 1.

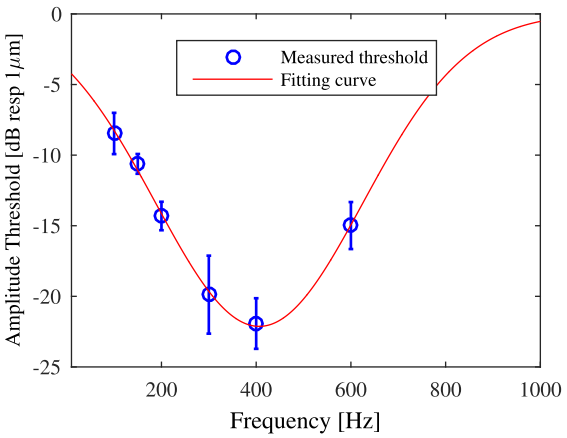

FIGURE 1. Interpolated amplitude thresholds (AT) based on experimental measurements of the five subjects listed in Table 1. The results are denoted by the blue circles with a standard error of the mean (SEM). The interpolated curve is described by $\log(AT(f)) = a + be^{-\frac{(f+c)^2}{d}}$ and was fitted using the parameters a, b, c, and d.

The values of $a(f)$ were fitted using the following equation based on the values of $a(f)$ listed in Table 1:

$$a(f) = kf + c, \tag{7}$$

where $a(f)$ is the exponent parameter with a unit response of 1 dB. The values of $a(f)$ after fitting are shown in Fig. 2.

Using these parameters, the power model was applied to evaluate the intensity of the vibration. The parameters of the stimuli, including the carrier frequency f_c, envelope frequency f_e, and intensity I are listed in Tables 2 to 4. The intensity I was calculated as follows:

$$I = I(f_c) + I(f_c - f_e) + I(f_c + f_e). \tag{8}$$

The experiment was based on three levels of intensity: $I = 25, 50$, and 75. To determine the displacement profiles of the stimuli, the displacement of the piezoelectric vibrator tip was measured using a laser displacement sensor (LK-H025, KEYENCE Corporation). The displacement was measured while there was no finger on the top of the actuator. Some examples of the stimuli are shown in Fig. 3. Because of the

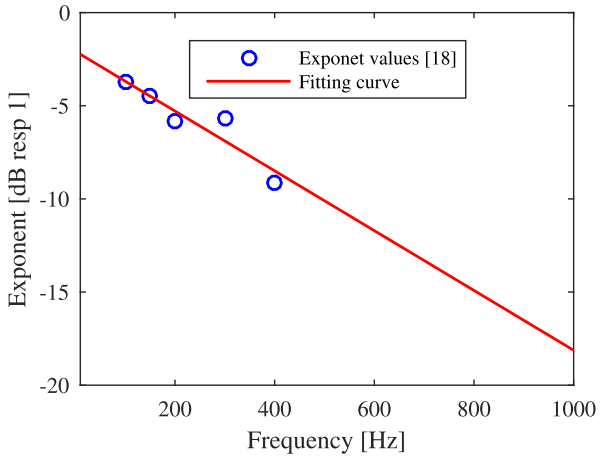

FIGURE 2. Exponent $a(f)$ [18] fitted using values listed in Table 1. The results are indicated by the blue circles and the fitting curve was based on the equation $a(f) = kf + c$, which was fitted using the parameters k and c.

TABLE 2. Stimuli parameters: pairs of stimuli comparing different intensities of sinusoidal and AM waveforms when $I_1 = I_2$.

Num	I_1	f_{c1}	f_{e1}	I_2	f_{c2}	f_{e2}
1	25	300	0	25	300	12
2	25	300	0	25	300	20
3	25	300	0	25	300	32
4	25	300	0	25	300	50
5	25	300	0	25	300	80
6	25	300	0	25	300	125
7	50	300	0	50	300	12
8	50	300	0	50	300	20
9	50	300	0	50	300	32
10	50	300	0	50	300	50
11	50	300	0	50	300	80
12	50	300	0	50	300	125
13	75	300	0	75	300	12
14	75	300	0	75	300	20
15	75	300	0	75	300	32
16	75	300	0	75	300	50
17	75	300	0	75	300	80
18	75	300	0	75	300	125

TABLE 3. Stimuli parameters: pairs of stimuli comparing the sinusoidal and AM waveforms of different carrier frequencies $f_{c1} \neq f_{c2}$.

Num	I_1	f_{c1}	f_{e1}	I_2	f_{c2}	f_{e2}
19	50	300	0	50	400	12
20	50	300	0	50	400	20
21	50	300	0	50	400	32
22	50	300	0	50	400	50
23	50	300	0	50	400	80
24	50	300	0	50	400	125
25	50	400	0	50	400	12
26	50	400	0	50	400	20
27	50	400	0	50	400	32
28	50	400	0	50	400	50
29	50	400	0	50	400	80
30	50	400	0	50	400	125

TABLE 4. Stimuli parameters: pairs of stimuli comparing AM waveforms with different carrier frequencies $f_{c1} \neq f_{c2}$ and different intensity levels.

Num	I_1	f_{c1}	f_{e1}	I_2	f_{c2}	f_{e2}
31	25	300	12	25	400	12
32	25	300	20	25	400	20
33	25	300	32	25	400	32
34	25	300	50	25	400	50
35	25	300	80	25	400	80
36	25	300	125	25	400	125
37	50	300	12	50	400	12
38	50	300	20	50	400	20
39	50	300	32	50	400	32
40	50	300	50	50	400	50
41	50	300	80	50	400	80
42	50	300	125	50	400	125
43	75	300	12	75	400	12
44	75	300	20	75	400	20
45	75	300	32	75	400	32
46	75	300	50	75	400	50
47	75	300	80	75	400	80
48	75	300	125	75	400	125

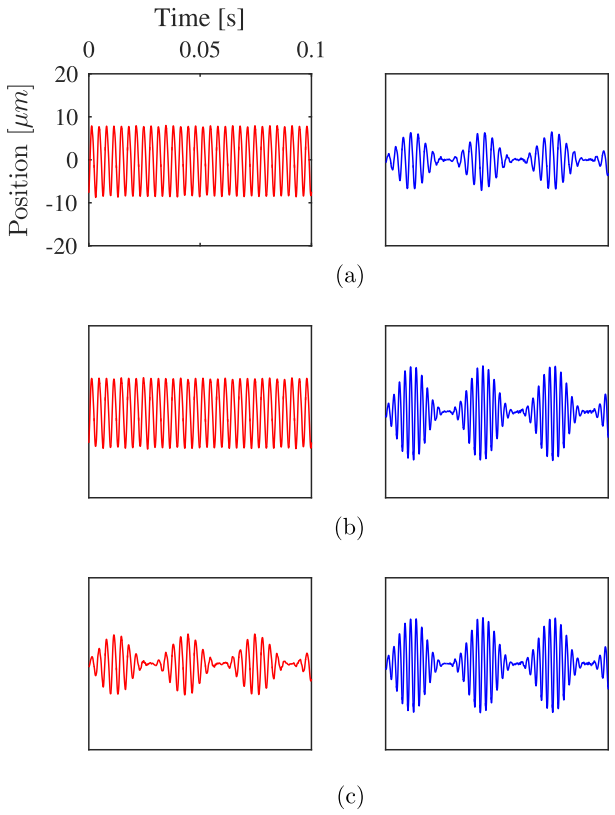

FIGURE 3. Examples of stimuli waves measured by the laser sensors. (a) Stimulus pair number 9 in Table 2. (b) Stimulus pair number 21 in Table 3. (c) Stimulus pair number 39 in Table 4.

large pushing and pulling forces (800 N and 50 N, respectively) of the actuator, it was assumed that the vibratory waveform did not change significantly between the preliminary measurements in which there was no contact force and the experiment during which the participants pressed their fingers on the actuator as instructed with a force of 0.5 N.

D. APPARATUS

The experimental apparatus is shown in Fig. 4 in which a tactile high-frequency vibration is generated by a piezo actuator (PZ12-112, Matsusada Precision) with pushing and pulling forces of 800 N and 50 N, respectively. The actuator contacts the finger of the subject through a 9-mm diameter hole in the plate. The diameter of the point of contact is 6 mm. The actuator is connected to a load cell (LUR-A-100NSA1, Kyowa Electronic Instruments) to measure the contact force, which is typically 0.5 N, between the actuator and a finger pad of a participant. The load cell is connected to a lab jack that is used to change the height of the actuator to adjust the contact force between the actuator and finger pad. A computer generates the input signal to the actuator through a USB audio interface (UR22mkII, Steinberg) and piezo driver (PZJRP6A, Matsusada Precision).

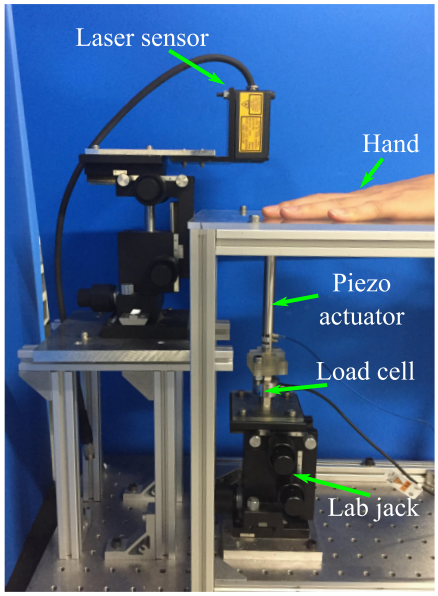

FIGURE 4. Subjects place their hand on the plate and contact the actuator with their finger.

E. PARTICIPANTS

The participants consisted of ten females and five males whose ages ranged from 20 to 28 years old. All participants used their dominant hand to perceive the stimuli in the experiments. Based on their self-reports, no participants suffered from motor or sensory limitations. While informed consent was obtained, the participants were unaware of the purpose of the experiment. The tasks of the participants were to discriminate the stimuli presented.

F. PROCEDURE

The three alternative forced-choice paradigm was selected to measure the discrimination ratio between the comparing vibrations. The 48 conditions listed in Tables 2 to 4 were adopted and 10 trials of each were conducted. A total of 480 trials were conducted for each participant.

In each trial, the participant received three stimuli in random order at 1-s intervals. Two of stimuli were the same as stimulus one while the other one was stimulus two. After all three stimuli were received, the participants were asked to identify which stimulus was different from others. After each set of 48 trials, the participants were allowed to rest for five to ten minutes.

Prior to the experiment, a piece of double-sided adhesive was affixed around the hole on the plate. The participants were instructed to press the center part of their index finger pad on the hole, and then to relax their hand on the plate. The lag jack holding the actuator was then slowly raised through the hole on the plate until it contacted the finger pad. The height of the actuator was adjusted until the expected contact force of 0.5 N was achieved between the finger and actuator. After each set of 48 trials, the double-sided adhesive tape was replaced, and the contact force was readjusted. Prior to the actual experiment, the participants completed 48 trials to familiarize themselves with the experimental procedure.

III. RESULTS

In this section, we derive the sensitivity d' as per the three-alternative forced-choice procedure to determine the ability to discriminate between the pairs of stimuli. The calculation procedure was based on the one described in [23]. A Kolmogorov–Smirnov test was conducted to confirm that all pairs of stimuli had normal distributions and the data was analyzed using a one-way analysis of variance (ANOVA) and a post-hoc analysis via a Tukey-Kramer test. The variance of the data quantified the sensitivity differences between the subjects. It is generally known that human sensitivity varies depending on the individual and it is understood that there may be individual variations in the boundaries detected. Even so, it is still possible to investigate the general trend in the sensation based on the results of a certain number of subjects, and this general trend is of particular interest in investigations of human sensitivity. In our experiment, there were a total of 15 subjects.

A. DISCRIMINATION BETWEEN SINUSOIDAL AND AM VIBRATIONS OF DIFFERENT INTENSITIES

Figures 5 to 7 show the values of d′ as per signal detection theory used to compare the stimuli in Table 2, which had intensities (I = 25, 50, or 75) and a carrier frequency (f_c = 300 Hz). Here, the various envelope frequencies were equally distributed on a logarithmic scale: f_{e1} = 0 and f_{e2} = 12, 20, 32, 50, 80, and 125 Hz. Humans possess two primary tactile receptors, namely, Meissner Corpuscles and Pacinian Corpuscles, which are sensitive to vibrations. The thresholds of the two receptors have a crossing frequency point around 40 Hz. The selection of envelope frequencies spans the crossing frequency of the two receptors. Based on the results, significant differences were observed between the envelope frequencies 12, 20, 32, 50, and 125 Hz. In contrast, no significant differences were observed between the envelope frequencies 80 and 125 Hz, which suggests that

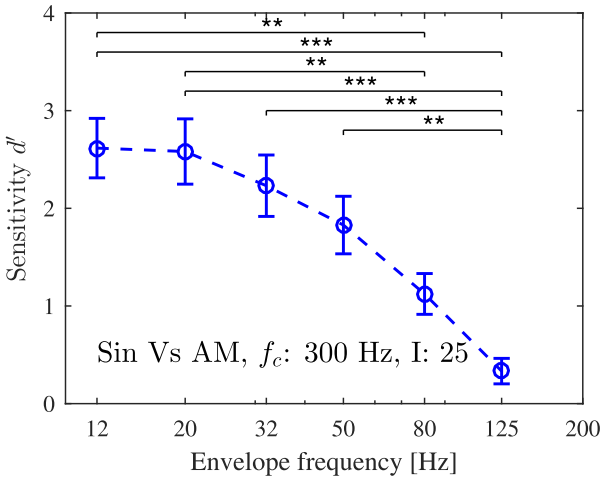

FIGURE 5. Sensitivity d′ of a comparison between stimuli with an envelope frequency f_{e1} = 0 Hz and different envelope frequencies f_{e2} from 12 to 125 Hz at an intensity I = 25. Here, *p < 0.05, **p < 0.01, and ***p < 0.001, and the error bars represent the SEM.

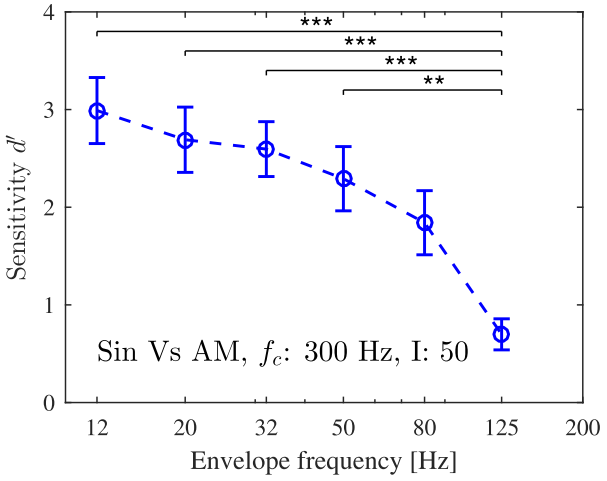

FIGURE 6. Sensitivity d' of a comparison between stimuli with an envelope frequency f_{e1} = 0 Hz and different envelope frequencies f_{e2} from 12 to 125 Hz at an intensity I = 50. Here, *p < 0.05, **p < 0.01, and ***p < 0.001, and the error bars represent the SEM.

the envelope frequency f_e = 80 Hz may be a discrimination boundary between the AM vibration ($f_e \neq 0$ Hz) and sinusoidal waveform ($f_e = 0$ Hz). A comparison of the three intensity levels is shown in Fig. 8 shows a comparison of the three intensity levels. The results shown in Fig. 8 indicate that there were significant differences between the d′ of intensity I = 25 and d′ of intensity I = 75 at an envelope frequency f_e = 80 Hz and between the d′ of intensity I = 25 and d′ of intensity I = 75 at an envelope frequency f_e = 125 Hz. The corresponding p-values were 0.0235 and 0.0012 respectively.

B. DISCRIMINATION BETWEEN SINUSOIDAL AND AM VIBRATIONS OF DIFFERENT CARRIER FREQUENCIES

As shown in Fig. 9, the d′ from signal detection theory was used to compare the stimuli in Table 3 that had the same

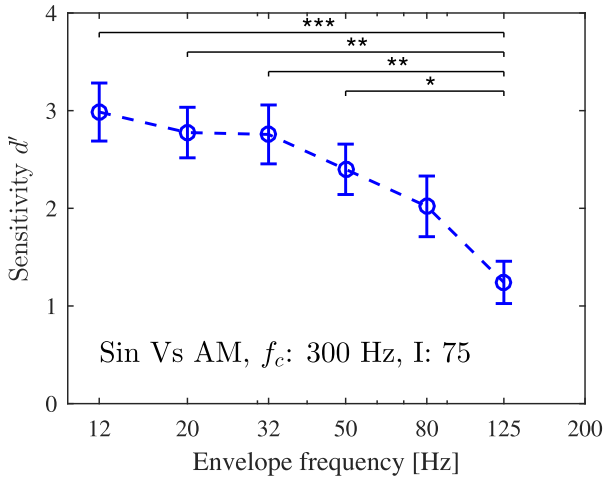

FIGURE 7. Sensitivity d' of a comparison between stimuli with an envelope frequency $f_{e1} = 0$ Hz and different envelope frequencies f_{e2} from 12 to 125 Hz at an intensity $I = 75$. Here, $^*p < 0.05$, $^{**}p < 0.01$, and $^{***}p < 0.001$, and the error bars represent the SEM.

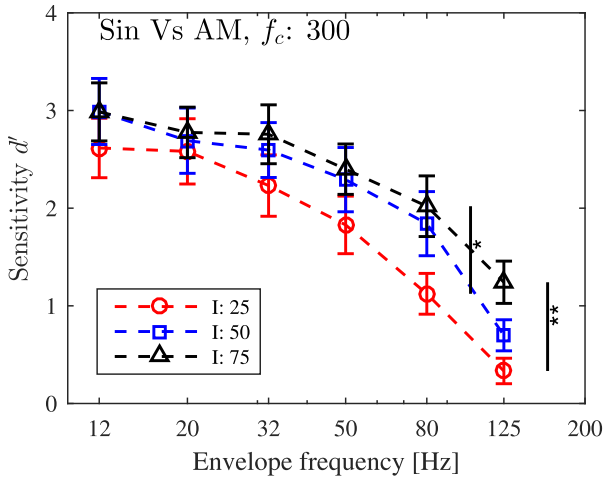

FIGURE 8. Sensitivity d' of a comparison between stimuli with an envelope frequency $f_{e1} = 0$ Hz and different envelope frequencies f_{e2} from 12 to 125 Hz and the same carrier frequency $f_c = 300$ Hz. The intensity were $I = 25$, 50 and 75. There were significant differences noted between $I = 25$ and $I = 75$ at $f_e = 80$ Hz and between the $I = 25$ and $I = 75$ at $f_e = 125$ Hz. Here, $^*p < 0.05$, $^{**}p < 0.01$, and $^{***}p < 0.001$, and the error bars represent the SEM.

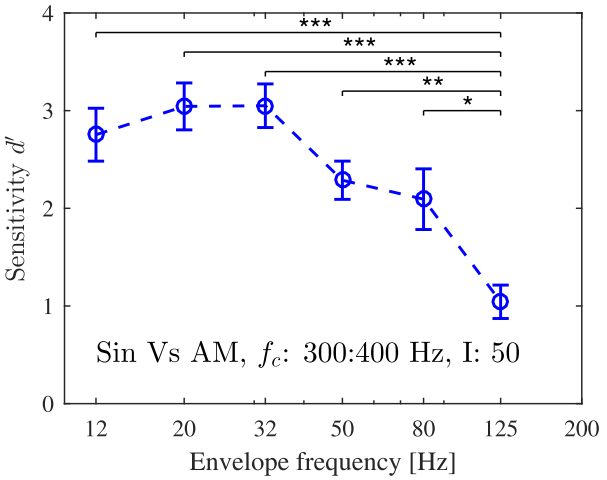

FIGURE 9. Sensitivity d' of a comparison between the stimuli with an envelope frequency $f_{e1} = 0$ Hz and different envelope frequencies f_{e2} from 12 to 125 Hz. The carrier frequencies were $f_{c1} = 300$ Hz vs $f_{c2} = 400$ Hz and the intensity was $I = 50$. Here, $^*p < 0.05$, $^{**}p < 0.01$, and $^{***}p < 0.001$, and the error bars represent the SEM.

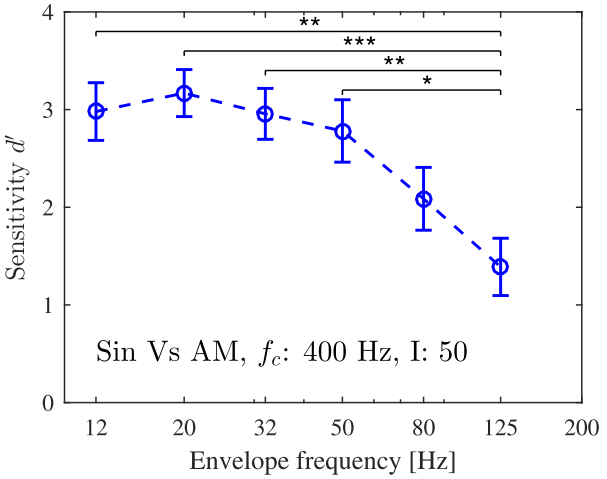

FIGURE 10. Sensitivity d' of a comparison between the stimuli with an envelope frequency $f_{e1} = 0$ Hz and different envelope frequencies f_{e2} from 12 to 125 Hz. The carrier frequency was $f_c = 400$ Hz, and the intensity was $I = 50$. Here, $^*p < 0.05$, $^{**}p < 0.01$, and $^{***}p < 0.001$, and the error bars represent the SEM.

intensity (I = 50), different carrier frequencies ($f_{c1} = 300$ Hz vs $f_{c2} = 400$ Hz), and different envelope frequencies of $f_{e1} = 0$ Hz and $f_{e2} = 12$, 20, 32, 50, 80, and 125 Hz. The carrier frequencies 300 Hz and 400 Hz were selected as they were much higher than the envelope frequency to ensure that the envelope signal was preserved in the stimuli as per Nyquist's law. The results show that significant differences were noted between envelope frequencies 12, 20, 32, 50, 80, and 125 Hz while no differences were noted between envelope frequencies 12, 20, 32, 50, and 80 Hz. Figure 10 depicts the d′ from signal detection theory used to compare the stimuli in Table 3 that had the same intensity (I = 50), different carrier frequencies ($f_{c1} = 300$ vs $f_{c2} = 400$), and different envelope frequencies of $f_{e1} = 0$ Hz and $f_{e2} = 12$, 20, 32, 50, 80, and 125 Hz, all of which were equally distributed on a logarithmic scale. The results showed that there were significant differences between the envelope frequencies 12, 20, 32, 50, and 125 Hz while no differences were observed between the envelope frequencies 12, 20, 32, 50, and 80 Hz or between 80 and 125 Hz. Figure 11 depicts a comparison among the different carrier frequencies in Figs. 5, 9, and 10. Significant differences were observed between $f_{c1} = f_{c2} = 300$ Hz and $f_{c1} = f_{c2} = 400$ Hz at an envelope frequency of $f_e = 125$ Hz.

C. DISCRIMINATION OF THE AM VIBRATION

Figure 12 shows the d′ values as per signal detection theory that were used to compare the stimuli in Table 4 that had the

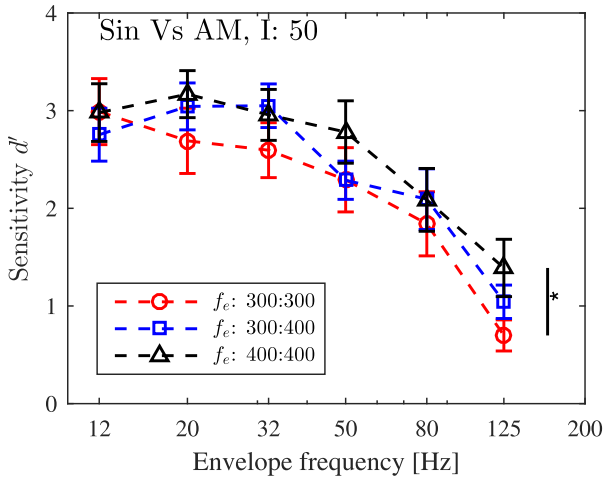

FIGURE 11. Sensitivity d' obtained from comparing the stimuli with an envelope frequency $f_{e1} = 0$ Hz and different envelope frequencies f_{e2} from 12 to 125 Hz. The carrier frequencies were $f_{c1} = f_{c2} = 300$ Hz, and $f_{c1} = 300$ Hz, $f_{c2} = 400$ Hz, and $f_{c1} = f_{c2} = 400$ Hz, which are represented by the red circles, blue squares, and black triangles, respectively. Significant differences were observed between $f_{c1} = f_{c2} = 300$ Hz and $f_{c1} = fc2 = 400$ Hz at $f_e = 125$ Hz. Here, *$p < 0.05$, **$p < 0.01$, and ***$p < 0.001$, and the error bars represent the SEM.

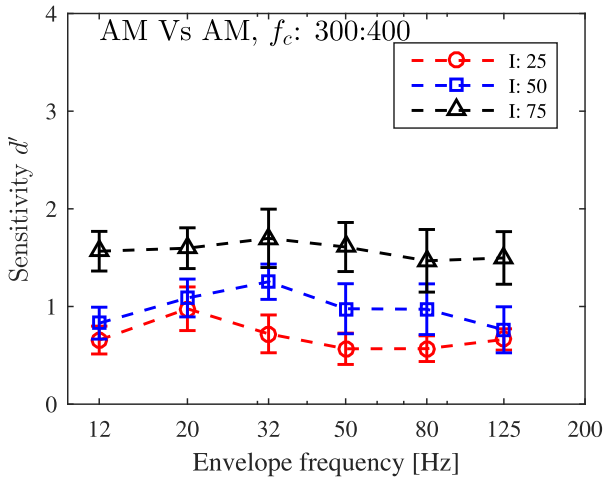

FIGURE 12. Sensitivity d' used in a comparison of the stimuli with envelope frequencies $f_{e1} = f_{e2}$ from 12 to 125 Hz and two carrier frequencies $f_{c1} = 300$ Hz vs $f_{c2} = 400$ Hz. The intensities were $I = 25$, 50, and 75, and are denoted with the red circles, blue squares, and black triangles, respectively. Here, *$p < 0.05$, **$p < 0.01$, and ***$p < 0.001$, and the error bars represent the SEM.

same intensities ($I = 25$, 50 or 75) and envelope frequencies ($f_{e1} = f_{e2}$) but different carrier frequencies ($f_{c1} = 300$ Hz vs $f_{c2} = 400$ Hz). No significant differences were noted among the envelope frequencies at each intensity. Figure 13 shows a comparison of the three intensity levels of Figure 12, where it can be seen that significant differences were observed between the d' at intensity $I = 25$ and d′ at intensity $I = 75$, and between the d′ at intensity $I = 50$ and d′ at intensity $I = 75$. The p-values in both of these cases were less than 0.001.

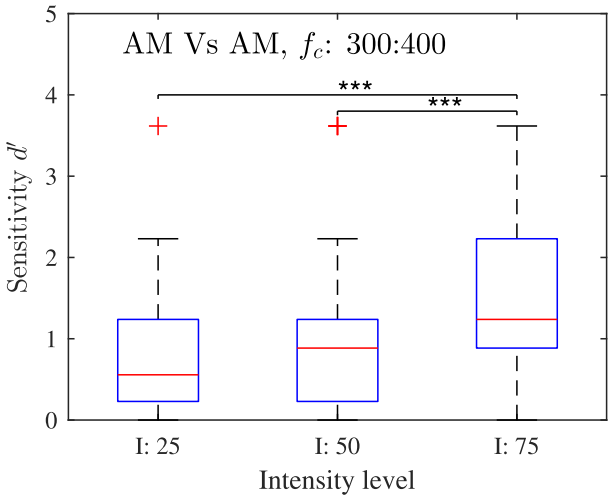

FIGURE 13. Sensitivity d' of a comparison between stimuli with the same envelope frequencies $f_{e1} = f_{e2}$ from 12 to 125 Hz and different carrier frequencies $f_{c1} = 300$ Hz vs $f_{c2} = 400$ Hz. The intensities were I = 25, I = 50, and I = 75. Here, *$p < 0.05$, **$p < 0.01$, and ***$p < 0.001$.

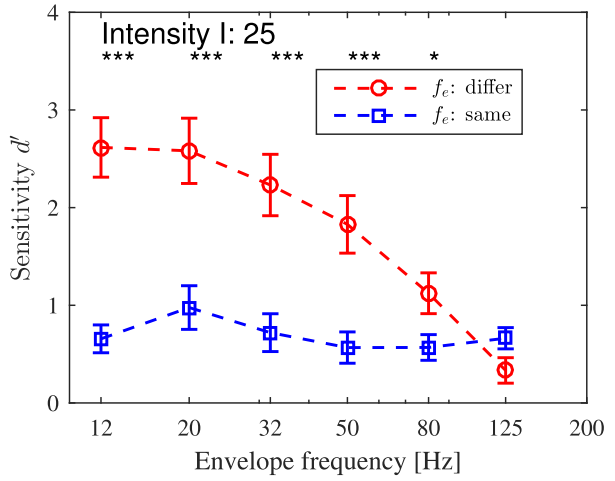

FIGURE 14. Sensitivity d' of a comparison between stimuli with envelope frequencies $f_{e1} = f_{e2}$ from 12 to 125 Hz. The cases for different envelope frequencies are denoted with red circles while those with the same envelope frequencies are denoted with blue squares. The carrier frequencies were $f_{c1} = f_{c2} = 300$ Hz and $f_{c1} = 300$ Hz, $f_{c2} = 400$ Hz, respectively, and the intensities were $I = 25$. Here, *$p < 0.05$, **$p < 0.01$, and ***$p < 0.001$, and the error bars represent the SEM.

D. COMPARING THE STIMULI WITH DIFFERENT ENVELOPES AND STIMULI WITH THE SAME ENVELOPE

Figures 14 to 16 depict the sensitivity d' values obtained from comparing stimuli with same envelope frequencies $f_{e1} = f_{e2}$ from 12 to 125 Hz and stimuli with different envelope frequencies $f_{e1} = 0$ Hz, f_{e2} from 12 to 125 Hz at intensities of $I = 25$, 50, and 75, respectively. The cases with different envelope frequencies f_e are denoted using the red circles while those that were the same are denoted using the blue squares. The carrier frequencies were $f_{c1} = f_{c2} = 300$ Hz,

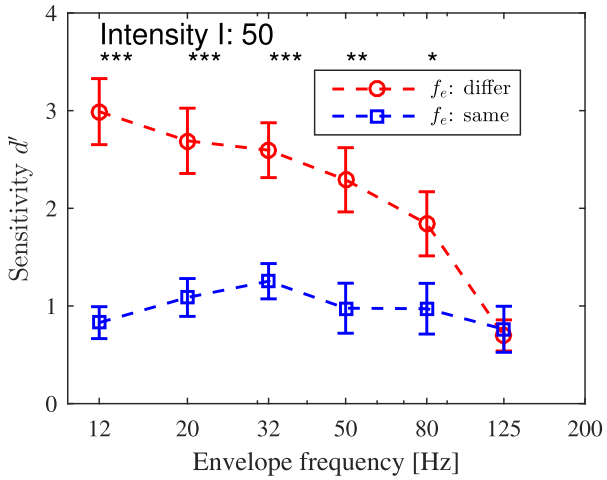

FIGURE 15. Sensitivity d' of a comparison between stimuli with envelope frequencies $f_{e1} = f_{e2}$ from 12 to 125 Hz. The cases with different envelope frequencies are denoted with red circles while those for the same envelope frequencies are denoted with blue squares. The carrier frequencies were $f_{c1} = f_{c2} = 300$ Hz and $f_{c1} = 300$ Hz, $f_{c2} = 400$ Hz, respectively, and the intensities were $I = 50$. Here, $^*p < 0.05$, $^{**}p < 0.01$, and $^{***}p < 0.001$, and the error bars represent the SEM.

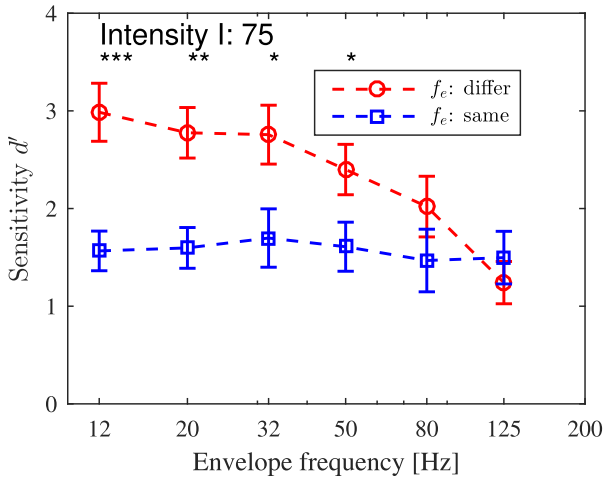

FIGURE 16. Sensitivity d' of a comparison between stimuli with envelope frequencies $f_{e1} = f_{e2}$ from 12 to 125 Hz. The cases with different envelope frequencies are denoted with red circles while those for the same envelope frequencies are denoted with blue squares. The carrier frequencies were $f_{c1} = f_{c2} = 300$ Hz and $f_{c1} = 300$ Hz, $f_{c2} = 400$ Hz, respectively, and the intensities were $I = 75$. Here, $^*p < 0.05$, $^{**}p < 0.01$, and $^{***}p < 0.001$, and the error bars represent the SEM.

and $f_{c1} = 300$ Hz, $f_{c2} = 400$ Hz, respectively. In this configuration, it was found that there were significant differences between the envelope frequencies 12, 20, 32, 50, and 80 Hz while no significant differences were observed for an envelope frequency of 125 Hz.

IV. DISCUSSION

A. PERCEPTION OF THE ENVELOPE FREQUENCY

Based on the results of the experiments, the perceptual discrimination of stimuli were found to have an envelope frequency dependence, as depicted in Figs. 5 to 8, and as the envelope frequency increased, the sensitivity of the vibration decreased. In [20], the threshold of the AM vibration was just below the threshold of the Meissner Corpuscle, which indicates the active of Meissner Corpuscle. In our results, the sensitivity was seen to drop as the envelope frequency increased. In the low envelope frequency region from 12 to 50 Hz, the sensitivity d' was found to be high, while in the high envelope frequency region from 80 to 125 Hz, the sensitivity d' was low. These results are similar to those for the active frequency range of the Meissner Corpuscle reported in [24]. The threshold of the Meissner Corpuscle, which is believed to be sensitive to the peak value of a waveform, reached its lowest point around 40 Hz but increased as the frequency increased. The threshold of the Pacinian Corpuscle, which is thought to be sensitive to the intensity of the waveform, was present above 10 Hz and reached its lowest point around 300 Hz. These two receptors overlap in frequency from 10 to 100 Hz. Comparing the threshold of the Meissner and Pacinian Corpuscles, below 40 Hz, the threshold of the Meissner Corpuscle is lower, while above 40 Hz, the amplitude threshold of the Pacinian Corpuscle is lower. Meissner Corpuscles are thought to be sensitive to the peak position, peak velocity, and the maximum of the product of the position and velocity below 100 Hz [16], [25]–[27], while Pacinian Corpuscles do not seem to be sensitive to the position and velocity but to the intensity or power of the stimuli above 100 Hz [4], [15]–[18], [28]. These results imply a lower envelope may be perceived by the Meissner Corpuscle when it is between 12 and 50 Hz, and the boundary for the envelope perception to be at an envelope frequency of around 80 to 125 Hz. At low envelope frequencies less than 50 Hz, the envelope perception of the vibration is straightforward. In our experiment, we did not investigate the envelope frequency in the range between 80 and 125 Hz and we also did not identify a specific boundary. However, the results showed that the sensitivity reached a low point when the envelope was 80 Hz or 125 Hz. Takenouchi *et al.* [14] modulated the original vibrotactile signal by maintaining the envelope of the transmitted vibration as they did not know envelope frequency range that should be maintained. Identifying the boundary above which the envelope begins to affect the discrimination of vibrations will prove useful when extracting the envelope signal of the modulation in teleoperation systems.

B. PERCEPTION OF THE INTENSITY

The intensity model works well for a high envelope frequency of 125 Hz; however, when the intensity is the same, it is difficult to discriminate vibrations. Intensity-based modeling [17] of the Pacinian Corpuscle typically assumes that identical intensities will be perceived as similar. At low envelope frequencies, discrimination is straightforward, which may be because they are within the active frequency range of the Meissner Corpuscle. In Figs. 5 to 8, it can be seen that there were significant differences between envelope frequencies of 12 to 50 Hz and 80 to 125 Hz and the sensitivity was

low at higher envelope frequency ranges where the activity of the Meissner Corpuscle is assumed to be weaker. From Figs. 14 to 16, no significant differences were observed between vibrations of stimuli with the same envelope and stimuli with different envelopes when the envelope frequency f_e was 125 Hz. The sensitivities d′ of high envelope frequencies were low but were not zero, which suggests that subjects were still somewhat able to discriminate. This may be due to the roughness of the intensity model. Our results also show that the sensitivity increased for high intensities, as shown in Figs. 8 and 13, which may suggest that the boundary of the envelope perception increased slightly as the intensity increased.

C. PERCEPTION OF CARRIER FREQUENCY

The carrier frequency was found to have a slight effect, as shown in Fig. 11, and significant differences only arose between $f_{c1} = f_{c2} = 300$ Hz and $f_{c1} = f_{c2} = 400$ Hz at an envelope frequency of $f_e = 125$ Hz. This suggests that the intensity information was significantly affected by the carrier frequency. In [4], [17], [18], and [28], superimposed vibrations or fine texture vibrations that did not contain distinct envelopes were used for discrimination. The intensity models in those studies could accurately predict the perceptual dissimilarities based on the intensity differences between the stimuli while the frequency of the stimuli did not significantly affect the discrimination. In our experiment, similar results were obtained. The sensitivity of comparing stimuli with different carrier frequencies showed a relative low d', which indicates that these stimuli were hard to discriminate. This may suggest that the carrier frequency of the vibration had only a minor effect on the perceptual discrimination. In previous studies, the discrimination of the carrier frequency difference was not fully investigated for cases where the stimuli had the same intensity. There is also a need to investigate the carrier effect over a larger frequency range. Note that the same intensity does not mean the same amplitude in terms of the displacement or acceleration.

D. LIMITATIONS OF THE STUDY

One possible limitation of the current study is that the employed intensity model was a relatively simple adaption of Equation 4. Even so, while other researchers have endeavored to identify more suitable models, such as the spectral minichannel model [17], it is possible that the simple intensity model is sufficient for our experiment as only two carrier frequencies were used. Another limitation is that we employed a simple type of AM vibration but did not consider any type of complex vibration. Thus, an area of future research will be to investigate whether complex waveforms exhibit tendencies similar to those obtained in this study. Finally, another limitation is that we measured the discrimination ability of a human index finger as we assumed that this was the most sensitive part of a human body. However, we did not evaluate the sensitivity of other parts, such as the feet and face. We assume that a lower envelope frequency boundary would be detected in other parts of the human body.

V. CONCLUSION

The intensity of high-frequency vibrations (i.e., vibrations $>$ 100 Hz) has been identified as a primary cue that can be used to convey vibrotactile information as per the Pacinian system. However, representative intensity models are insufficient when interpreting the perception of the envelope of high-frequency vibrations as the intensity and envelope together affect the ability of humans to discriminate high-frequency vibrations.

The objective of the current study was to identify the boundary frequency of the envelope sensation. We conducted an experiment to assess the discrimination ability of subjects exposed to AM and sinusoidal vibrations of different envelope frequencies, carrier frequencies, and intensity levels using an intensity model developed in previous studies. In our testing, we investigated the effect of the intensity and envelope on the ability of humans to discriminate high-frequency vibrations, and our results suggest that the boundary of the envelope perception was at an envelope frequency of around 80 to 125 Hz and at envelope frequencies below 50 Hz. In these ranges, the envelope perception of the vibration is straightforward. In addition, we found the effect of the carrier frequency on the discrimination was small, and the discrimination ability of envelope and carrier frequency tended to increase as the intensity increased.

REFERENCES

[1] A. M. Okamura, M. R. Cutkosky, and J. T. Dennerlein, "Reality-based models for vibration feedback in virtual environments," *IEEE/ASME Trans. Mechatronics*, vol. 6, no. 3, pp. 245–252, Sep. 2001.
[2] K. Higashi, S. Okamoto, and Y. Yamada, "What is the hardness perceived by tapping?" in *Proc. Int. Conf. Hum. Haptic Sens. Touch Enabled Comput. Appl.*, 2016, pp. 3–12.
[3] K. J. Kuchenbecker, J. Fiene, and G. Niemeyer, "Improving contact realism through event-based haptic feedback," *IEEE Trans. Vis. Comput. Graphics*, vol. 12, no. 2, pp. 219–230, Mar. 2006.
[4] S. J. Bensmaia and M. Hollins, "The vibrations of texture," *Somatosensory Motor Res.*, vol. 20, no. 1, pp. 33–43, 2003.
[5] W. McMahan *et al.*, "Tool contact acceleration feedback for telerobotic surgery," *IEEE Trans. Haptics*, vol. 4, no. 3, pp. 210–220, May 2011.
[6] J. M. Romano and K. J. Kuchenbecker, "Creating realistic virtual textures from contact acceleration data," *IEEE Trans. Haptics*, vol. 5, no. 2, pp. 109–119, Apr. 2012.
[7] W. McMahan, J. M. Romano, A. M. A. Rahuman, and K. J. Kuchenbecker, "High frequency acceleration feedback significantly increases the realism of haptically rendered textured surfaces," in *Proc. IEEE Haptics Symp.*, Mar. 2010, pp. 141–148.
[8] T. Ahmaniemi, J. Marila, and V. Lantz, "Design of dynamic vibrotactile textures," *IEEE Trans. Haptics*, vol. 3, no. 4, pp. 245–256, Oct. 2010.
[9] S. Wu, X. Sun, Q. Wang, and J. Chen, "Tactile modeling and rendering image-textures based on electrovibration," *Vis. Comput.*, vol. 33, no. 5, pp. 637–646, 2017.
[10] B.-A. J. Menelas and M. J.-D. Otis, "Design of a serious game for learning vibrotactile messages," in *Proc. IEEE Int. Workshop Haptic Audio Vis. Environ. Games (HAVE)*, Oct. 2012, pp. 124–129.
[11] M. Konyo, H. Yamada, S. Okamoto, and S. Tadokoro, "Alternative display of friction represented by tactile stimulation without tangential force," in *Proc. Int. Conf. Hum. Haptic Sens. Touch Enabled Comput. Appl.*, 2008, pp. 619–629.

[12] T. Ahmaniemi, "Effect of dynamic vibrotactile feedback on the control of isometric finger force," *IEEE Trans. Haptics*, vol. 6, no. 3, pp. 376–380, Jul. 2013.
[13] A. M. Murray, R. L. Klatzky, and P. K. Khosla, "Psychophysical characterization and testbed validation of a wearable vibrotactile glove for telemanipulation," *Presence, Teleoper. Virtual Environ.*, vol. 12, no. 2, pp. 156–182, 2003.
[14] H. Takenouchi, N. Cao, H. Nagano, M. Konyo, and S. Tadokoro, "Extracting haptic information from high-frequency vibratory signals measured on a remote robot to transmit collisions with environments," in *Proc. IEEE/SICE Int. Symp. Syst. Integr. (SII)*, Dec. 2017, pp. 968–973.
[15] J. C. Makous, R. M. Friedman, and C. J. Vierck, "A critical band filter in touch," *J. Neurosci.*, vol. 15, no. 4, pp. 2808–2818, 1995.
[16] S. J. Bensmaıa and M. Hollins, "Complex tactile waveform discrimination," *J. Acoust. Soc. Amer.*, vol. 108, no. 3, pp. 1236–1245, 2000.
[17] S. Bensmaıa, M. Hollins, and J. Yau, "Vibrotactile intensity and frequency information in the Pacinian system: A psychophysical model," *Attention, Perception, Psychophys.*, vol. 67, no. 5, pp. 828–841, 2005.
[18] S. Bensmaıa and M. Hollins, "Pacinian representations of fine surface texture," *Perception Psychophys.*, vol. 67, no. 5, pp. 842–854, 2005.
[19] S.-C. Lim, K.-U. Kyung, and D.-S. Kwon, "Effect of frequency difference on sensitivity of beats perception," *Exp. Brain Res.*, vol. 216, no. 1, pp. 11–19, 2012.
[20] P. J. J. Lamoré, H. Muijser, and C. Keemink, "Envelope detection of amplitude-modulated high-frequency sinusoidal signals by skin mechanoreceptors," *J. Acoust. Soc. Amer.*, vol. 79, no. 4, pp. 1082–1085, 1986.
[21] Y. Makino, T. Maeno, and H. Shinoda, "Perceptual characteristic of multispectral vibrations beyond the human perceivable frequency range," in *Proc. IEEE World Haptics Conf. (WHC)*, Jun. 2011, pp. 439–443.
[22] G. Park and S. Choi, "Perceptual space of amplitude-modulated vibrotactile stimuli," in *Proc. IEEE World Haptics Conf. (WHC)*, Jun. 2011, pp. 59–64.
[23] L. T. DeCarlo, "On a signal detection approach to m-alternative forced choice with bias, with maximum likelihood and Bayesian approaches to estimation," *J. Math. Psychol.*, vol. 56, no. 3, pp. 196–207, 2012.
[24] S. J. Bolanowski, Jr., G. A. Gescheider, R. T. Verrillo, and C. M. Checkosky, "Four channels mediate the mechanical aspects of touch," *J. Acoust. Soc. Amer.*, vol. 84, no. 5, pp. 1680–1694, Nov. 1988.
[25] F. J. Looft, "Response of monkey glabrous skin mechanoreceptors to random-noise sequences: I. Temporal response characteristics," *Somatosensory Motor Res.*, vol. 11, no. 4, pp. 327–344, 1994.
[26] F. J. Looft, "Response of monkey glabrous skin mechanoreceptors to random noise sequences: Ii. dynamic stimulus state analysis," *Somatosensory Motor Res.*, vol. 13, no. 1, pp. 11–28, 1996.
[27] F. J. Looft, "Response of monkey glabrous skin mechanoreceptors to random noise sequences: III. Spectral analysis," *Somatosensory Motor Res.*, vol. 13, nos. 3–4, pp. 235–244, 1996.
[28] T. Yoshioka, S. J. Bensmaia, J. C. Craig, and S. S. Hsiao, "Texture perception through direct and indirect touch: An analysis of perceptual space for tactile textures in two modes of exploration," *Somatosensory Motor Res.*, vol. 24, nos. 1–2, pp. 53–70, 2007.

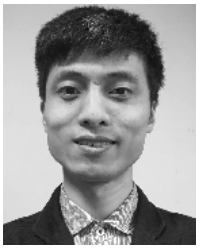

NAN CAO (S'17) received the B.S. degree in electronics science and technology (optical electronics) and the M.S. degree in optical engineering from the Beijing Institute of Technology, Beijing, China, in 2012 and 2015, respectively. He is currently pursuing the Ph.D. degree with the Department of Applied Information Sciences, Tohoku University.

MASASHI KONYO (M'05) received the B.S., M.S., and Ph.D. degrees in engineering from Kobe University, in 1999, 2001, and 2004, respectively.

He is currently an Associate Professor with the Graduate School of Information Sciences, Tohoku University. His research interests include haptic interfaces, rescue robotics, and new actuators. He was a recipient of the Young Scientists Prize, a Commendation for Science and Technology by MEXT in 2015, the Best Paper Award from the *Journal of Robotics and Mechatronics*, in 2010, and *Advanced Robotics*, in 2016, the Best Poster Award of the World Haptics Conference, in 2007 and 2013, and the Best Hands on Demo Award at the Euro-Haptics 2008 and the Haptics Symposium 2014.

HIKARU NAGANO received the B.S., M.S., and Ph.D. degrees in engineering from Nagoya University, in 2010, 2012, and 2015, respectively. He was an Assistant Professor with Tohoku University, from 2015 to 2018. He is currently an Assistant Professor with the Graduate School of Engineering, Kobe University. His research interests include human haptic perception and human–machine interfaces.

SATOSHI TADOKORO was an Associate Professor with Kobe University, from 1993 to 2005. He is currently a Professor with the Graduate School of Information Sciences, Tohoku University. Since 2014, he has been a Project Manager of the ImPACT Project of the Japanese Government. He was the Project Leader of the MEXT DDT Project on rescue robotics, from 2002 to 2007, and developed Quince, a UGV for CBRNE disasters that were used in the Fukushima–Daiichi Nuclear Power Plant response, in 2011. He established RoboCup Rescue, in 1999, the IEEE Robotics and Automation Society (RAS) TC on Safety, Security, and Rescue Robotics, in 2001, and the International Rescue System Institute, in 2002. He was the President of the IEEE RAS, from 2016 to 2017.